IOSR Journal of Electrical and Electronics Engineering (IOSR-JEEE)
e-ISSN: 2278-1676, p-ISSN: 2320-3331, Volume 16, Issue 4 Ser. I (Jul. – Aug. 2021), PP 09-18
www.iosrjournals.org

Simulation of High Step-Up Isolated Interleaved Converter for Renewable Energy System

Koyyana Srinivasa Rao[1], V.R.S.Divy[2] N.Sandhya Rani[2] P.V.Srikar[2] R.Ravi[2]
[1](Asst.professor, Dept. of EEE, Lendi institute of engineering and technology, AP, India)
[2](Students, Dept. of EEE, Lendi institute of engineering and technology, AP, India)

Abstract: *A new high step-up converter, which is suitable for renewable energy system, is proposed in this paper. Through a Voltage multiplier module composed of switched capacitors and coupled inductors, a conventional interleaved boost converter obtains high step-up gain without operating at extreme duty ratio. The configuration of the proposed converter not only reduces the current stress but also constrains the input current ripple, which decreases the conduction losses and lengthens the life time of the input source. In addition, due to the loss less passive clamp performance, leakage energy is recycled to the output terminal. Hence, large voltage spikes across the main switches are alleviated, and the efficiency is improved. Even the low voltage stress makes the low-voltage-rated MOSFETs be adopted for reductions of conduction losses and cost. An additional battery control is added to the input renewable energy system to work as a back up storage system with reduces the variations in the output waveform*

Key Word: *interleaved converter, solar, Battery control.*

Date of Submission: 28-06-2021 Date of Acceptance: 12-07-2021

I. Introduction

Recently, photovoltaic (PV) power-generation systems are increasingly important and prevalent in distribution generation systems. A conventional centralized PV array is a serial connection of Numerous panels to obtain higher DC-link voltage for main electricity through a DC-AC inverter Unfortunately, once there is a partial shadow on some panels, the system's energy yield Becomes significantly reduced. An AC module is a micro inverter configured on the rear bezel of a PV panel this alternative solution not only immunizes against the yield loss by shadow effect, but also provides flexible installation options according to the user's budget Many prior research work shave proposed a single-stage DC-AC inverter with fewer components to fit the dimensions of the bezel of the AC module, but their efficiency levels are lower than those of conventional PV inverters. The power capacity range of a single PV panel is about 100 W to 300 W, and the maximum power point (MPP) voltage range is from 15 V to 40 V, which will be the input voltage of the AC module; in cases with lower input voltage, it is difficult for the AC module to reach high efficiency. However, employing a high step-up DC-DC converter in the front of the inverter improves power-conversion efficiency and provides a stable DC link to the inverter. When installing the PV generation system during daylight, for safety reasons, the AC module outputs zero voltage shows the solar energy through the PV panel and micro inverter to the output terminal when the switches are off. When a worker is installing the AC module, this potential difference could pose hazards to the human body or facilities. A floating active switch is designed to isolate the DC current from the PV panel, for when the AC module is off-grid as well as in then on-operating condition. This isolation ensures the operation of the internal components without any residential energy being transferred to the output or input terminals, which could be un safe. The micro inverter includes DC-DC boost converter, DC-AC inverter with control circuit. The DC-DC converter requires large step-up conversion from the panel's low voltage to the voltage level of the application. Previous research on various converters for high step-up applications has included analyses of the switched-inductor and switched-capacitor types; transformer less switched-capacitor type the voltage-lift type the capacitor-diode voltage multiplier and the boost type integrated with a coupled inductor , these converters by increasing turns ratio of coupled inductor obtain higher voltage gain than conventional boost converter. Some converters successfully combined boost and fly back converters, since various converter combinations are developed to carry out high step-up voltage gain by using the coupled-inductor technique. The efficiency and voltage gain of the DC-DC boost converter are constrained by either the parasitic effect of the power switches or the reverse-recover issue of the diodes. In addition, the equivalent series resistance (ESR) of the capacitor and the parasitic resistances of the inductor also affect overall efficiency. Use of active clamp technique not only recycles the leakage inductor's energy but also constrain the voltage stress across the active switch , how ever the tradeoff is higher cost and complex control circuit. By combine active snubber, auxiliary resonant circuit, synchronous rectifiers, or switched- capacitor-based resonant

circuits and so on, these techniques made active switch into zero voltage switching (ZVS) or zero current switching (ZCS) operation and improved converter efficiency. However, when the leakage-inductor energy from the coupled inductor can be recycled, the voltage stress on the active switch is reduced, which means the coupled inductor employed in combination with the voltage-multiplier or voltage-lift technique successfully accomplishes the goal of higher voltage gain.

The proposed converter, is comprised of a coupled inductor *T1* with the floating active switch *S*1. The primary winding *N*1 of a coupled inductor *T1* is similar to the input inductor of the conventional boost converter, and capacitor *C1* and diode *D1* receive leakage inductor energy from *N*1. The secondary winding *N*2 of coupled inductor *T1* is connected with another pair of capacitors *C2* and diode *D2*, which are in series with *N*1 in order to further enlarge the boost voltage. The rectifier diode *D3*connects to its output capacitor *C3*. The proposed converter has several features: 1) the connection of the two pairs of inductors, capacitor and diode give a large step-up voltage-conversion ratio; 2) the leakage-inductor energy of the coupled inductor can be recycled, thus increasing the efficiency; and the voltage stress across the active switch is restrained; and 3) the floating active switch efficiently isolates the PV panel energy during non-operating conditions, which enhances facility and human safety.

Hybrid electric vehicles have recently achieved significant market penetration and stimulated a great amount of research work. Cost-effective high-efficiency integrated power-electronic modules are one of the key elements toward making practical electric propulsions to control the electric-drive motors. The reliability of these power modules is of paramount importance for the commercial success of various types of electric vehicles. Electric-drive trains, due to their wide dynamic range of operation and diverse, impose a stringent reliability requirement on the power modules than any other industrial motor-control applications.

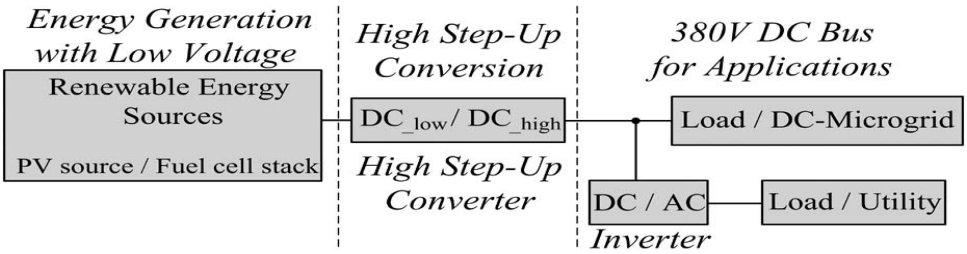

Fig. 1. Typical renewable energy system.

As above fig, a typical power module has hundreds of wire bonds and numerous solder joints, which are subject to thermo mechanical stress and fatigue caused by unavoidable power dissipation in the module. The reliability of power semiconductor Modules has been a concern for many industrial Systems, particularly for the railway-traction applications in Europe and Japan, since their market introduction in early1990s. Module failures are reported in literature both during power-cycling testing and in field usage . Wire-bond lift-off and cracks at silicon-substrate or substrate-base plate solder joints have been identified as the main failure mechanisms. Different operation conditions of the inverters result in varied inverter-phase current and power dissipation. This results in thermo mechanical stress and fatigue. Power modules can and will fail, given enough stress and time. However, power modules usually go through a gradual degradation process before catastrophic failure occurs. The degradation process shows some early symptoms on the state of health (SoH) of these power modules, including an increase in forward on-voltage, leakage current, thermal impedance, and, possibly, small signal Impedance and noise level. The purpose of this paper is to develop an online diagnostic and prognostic system in electric, hybrid electric, and fuel cell vehicles to warn the driver of potential failure of the power-electronic modules. Online diagnostics and condition. Monitoring was used in induction and brushless dc motors, as well as internal combustion engines. Yet, no work was reported to apply this approach in monitoring the SoH of power modules. In this paper, we first conducted a parametric investigation of power-module degradation processes. A computer-controlled stress test system was developed. Parametric measurement was taken periodically during the power-module stress testing. The measurement results were then analyzed to identify early warning signatures, which were used to provide onboard prognostic capability to monitor the SoH of power modules. Due to the complexity of deterioration mechanisms and the widespread parameter distribution of power modules, we have developed a practical algorithm to implement the prognostic function, to judge whether a power module is on the verge of failing or in a good condition. The algorithm has been verified with extensive Simulink modeling. In the past century, global surface temperatures have increased at a rate near 0.6 ◦C/century because of global warming caused by effluent gas emissions and increases in CO_2 levels in the atmosphere. The problems with energy Supply and use are related not only to global warming but also to such environmental concerns as air pollution, acid precipitation, ozone depletion, forest destruction, and

radioactive substance emissions. To prevent these effects, some potential solutions have evolved including energy conservation through improved energy efficiency, a reduction in fossil fuel use and an increase in environmentally friendly energy supplies. Recently, energy Generated from clean, efficient and environmentally-friendly sources has become one of the major challenges for engineers and scientists. Among them, the photovoltaic (PV) generation system has received great attention in research because it appears to be one of the possible solutions to the environmental problem. Recently, dc–dc converters with high voltage gain have become usually required in many industrial applications such as the front-end stage for clean-energy sources, the dc back-up energy system for uninterruptible power supply, high-intensity discharge lamps for automobile headlamps, and telecommunication Industry applications.

The conventional boost converters cannot provide such a high dc voltage gain, even for an extreme duty cycle. It also may result in serious reverse recovery problem and increase the rating of all devices. As a result, the conversion efficiency is degraded and the electromagnetic interference problem is severe under this situation. To increase the conversion efficiency and voltage gain, many modified step-up converter topologies have been Investigated in the past decades Although voltage clamped techniques are manipulated in the converter design to overcome the severe reverse-recovery problem of the output diode in high-level voltage applications, there still exist overlarge switch voltage stresses and the voltage gain is limited by the turn-on time of the auxiliary switch Wai and Duan investigated a novel coupled-inductor converter strategy to increase the voltage gain of a conventional boost converter with a single inductor, and deal with the problem of the leakage inductor and demagnetization of the transformer in a conventional coupled-inductor-based converter. In this paper, the high step-up converter topology in is introduced to boost and stabilize the output dc voltage of PV modules for the utilization of a dc–ac inverter. Developments in microelectronics and power devices have caused the widespread application of pulse width-modulation(PWM) inverters in industries. The basic mechanism of a PWM inverter is to convert the dc voltage to a sinusoidal ac output through the inverter-*LC* filter blocks. The performance is evaluated by the total harmonic distortion (THD), the transient response, and the efficiency. Thus, much attention has been paid to the closed-loop regulation of PWM inverters to achieve good dynamic response under different types of loads in the past decade, e.g., linear control, observer for grid current control, Lyapunov-based control sliding-mode control(SMC) etc. Variable structure control with sliding mode, or SMC, is one of the effective nonlinear robust control approaches since it provides system dynamics with an invariance Property to uncertainties once the system dynamics are controlled in the sliding mode. The insensitivity of the controlled system to uncertainties exists in the sliding mode, but not during the reaching phase, i.e., the system dynamic in the reaching phase is still influenced by uncertainties. Recently some researchers have adopted the idea of total SMC (TSMC)to get a sliding motion through the entire state trajectory, i.e., no reaching phase exists in the control process ,so that the controlled system through the whole control processes not influenced by uncertainties. This paper attempts to extend an adaptive TSMC (ATSMC) from to the voltage control of a PWM inverter. Up to now, this is the first time that the application of TSMC to the power electronics control is investigated. In general, the output power of a PV module is substantially changed according to different irradiations. For example, in Taiwan, the direction with the maximum average irradiations during the year is South and the corresponding angle of inclinations 23.5◦ so that many PV modules are installed in this posture. However, the maximum irradiations cannot be captured persistently in this way such that the performance of the PV generation system cannot be improved effectively. Recently, many researchers have made efforts in sun tracking investigations. The conventional sun tracking strategies equip light sensors on the terminals of PV plates. When the feedback signals from light sensors are equal, it means that the PV plate faces the sun and has the maximum irradiation at the corresponding position. Unfortunately, the initial proofreading and correcting of light sensors are time consuming and the device properties are easily varied under different operational conditions. In order to overcome the aforementioned drawbacks, this paper investigates an active sun tracking scheme without light sensors via the property of the open circuit voltage of PV modules proportional to the corresponding irradiation to follow the trail of the sun.The topic of this paper focuses on the development of a high performance stand-alone PV generation system. It contains three main contents including a high step-up converter, a PWM inverter with ATSMC, and an active sun tracking scheme. First, the active sun-tracking scheme is designed to capture maximum irradiation and powers. Then, the high step-up converter is implemented for converting the captured power from the active sun-tracking scheme to form a stable dc voltage source. In addition, the PWM inverter with ATSMC transfers this dc voltage source from the high step-up converter into an ac voltage source for stand-alone utilization.

II. Interleaved Converter

The proposed high step-up interleaved converter with a voltage multiplier module is shown in Fig. 2. The voltage multiplier module is composed of two coupled inductors and two switched capacitors and is inserted between a conventional interleaved boost converter to form a modified boost–flyback–forward interleaved structure. When the switches turn off by turn, the phase whose switch is in OFF state performs as a flyback converter, and the other phase whose switch is in ON state performs as a forward converter.

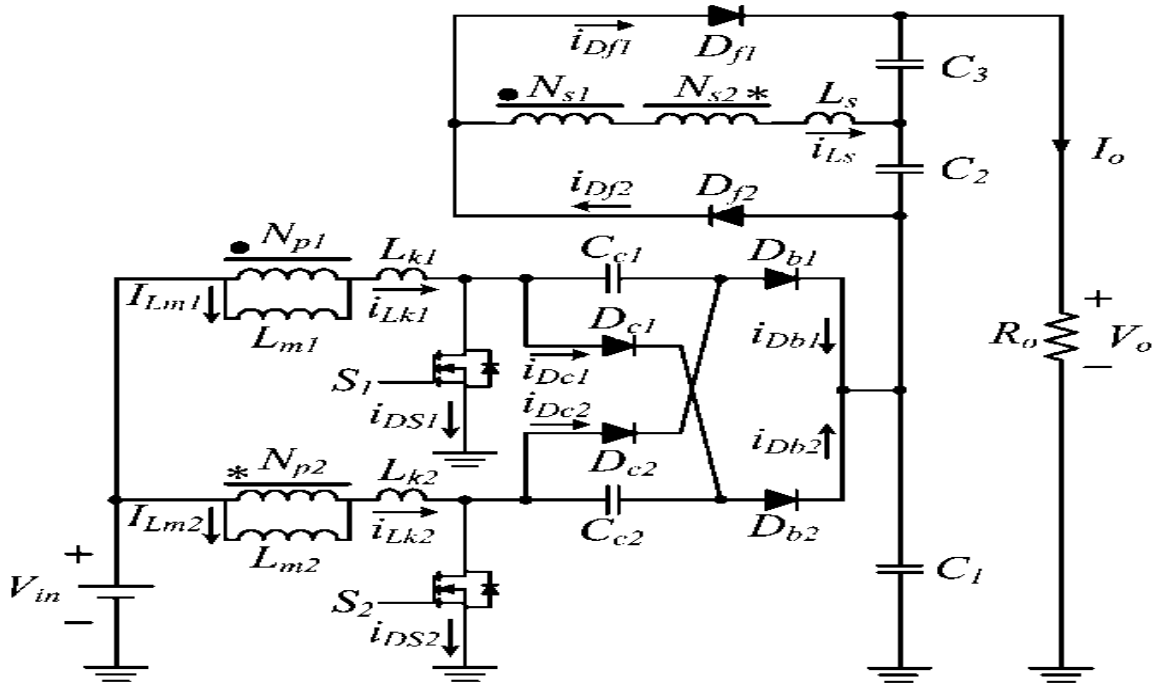

Fig 2 Isolated interleaved converter.

Mode I [t_0, t_1]: At *t=t0*, the power switch *S2* remains on-state, and other power switch *S1* begins to turn on. The diodes *Dc1*, *Dc2*, *Db1*, *Db2* and *Df1* are reversed-biased, as shown in Fig. 2.3 (a). The series leakage inductors *Ls* quickly releases the stored energy to output terminal via flyback-forward diode *Df2*, and the current through series leakage inductors *Ls* decreases to zero. Thus, the magnetizing inductor *Lm1* still transfers energy to secondary side of coupled inductors. The current through leakage inductor *Lk1* increases linearly, and other current through leakage inductor *Lk2* decreases linearly.

Mode II [*t1*, *t2*]: At *t=t1*, both of the power switches *S1* and *S2* remain on-state, and all diodes are reversed-biased, as shown in Fig. 5(b). Both currents though leakage inductors *Lk1* and *Lk2*, are increase linearly due to charging by input voltage source *Vin*.

Mode III [*t2*, *t3*]: At *t=t2*, the power switch *S1* remains on-state, and other power switch *S2* begins to turn off. The diodes *Dc1*, *Db1* and *Df2* are reversed-biased, as shown in Fig. 5(c). The energy stored in magnetizing inductor *Lm2* transfers to secondary side of coupled inductor, and the current through series leakage inductors *Ls* flows to output capacitor *C3* via flyback-forward diode *Df1*. The voltage stress on power switch *S2* is clamped by clamp capacitor *Cc1* which equals output voltage of boost converter. The input voltage source, magnetizing inductor *Lm2*, leakage inductor *Lk2* and clamp capacitor *Cc2* release energy to output terminal, thus V*C1* obtains a double output voltage of boost converter.

Mode IV [*t3*, *t4*]: At *t=t3*, the current *iDc2* has naturally decreased to zero due to the magnetizing current distribution, and hence diode reverse recovery losses are alleviated and conduction losses are decreased. Both power switches and all diodes remain previous states except the clamp diode *Dc2*, as shown in Fig. 5(d).

Mode V [*t*4, *t*5]*:* At *t* = *t*4, the power switch *S*1 remains in ON state, and the other power switch *S*2 begins to turn on. The diodes *Dc*1, *Dc*2, *Db*1, *Db*2, and *Df*2 are reversed biased, as shown in Fig. 5(e). The series leakage inductors *Ls* quickly release the stored energy to the output terminal via flyback–forward diode *Df*1, and the current through series leakage inductors decreases to zero. Thus, the magnetizing inductor *Lm*2 still transfers energy to the secondary side of coupled inductors. The current through leakage inductor *Lk*2 increases linearly, and the other current through leakage inductor *Lk*1 decreases linearly.

Mode VI [*t*5, *t*6]*:* At *t* = *t*5, both of the power switches *S*1 and *S*2 remain in ON state, and all diodes are reversed biased, as shown in Fig. 5(f). Both currents through leakage inductors *Lk*1 and *Lk*2 are increased linearly due to charging by input voltage source *V*in.

Mode VII [*t*6, *t*7]*:* At *t* = *t*6, the power switch *S*2 remains in ON state, and the other power switch *S*1 begins to turn off. The diodes *Dc*2, *Db*2, and *Df*1 are reversed biased, as shown in Fig. 5(g). The energy stored in magnetizing inductor *Lm*1 transfers to the secondary side of coupled inductors, and the current through series leakage inductors flows to output capacitor *C*2 via flyback–forward diode *Df*2. The voltage stress on powerswitch *S*1 is clamped by clamp capacitor *Cc*2 which equals theoutput voltage of the boost converter. The input voltage source, magnetizing inductor *Lm*1, leakage inductor *Lk*1, and clamp capacitor *Cc*1 release energy to the output terminal; thus, *VC*1 obtains double output voltage of the boost converter.

Mode VIII [*t*7, *t*8]*:* At *t* = *t*7, the current *iDc*1 has naturally decreased to zero due to the magnetizing current distribution, and hence, diode reverse recovery losses are alleviated and conduction losses are decreased. Both power switches and all diodes remain in previous states except the clamp diode *Dc*1

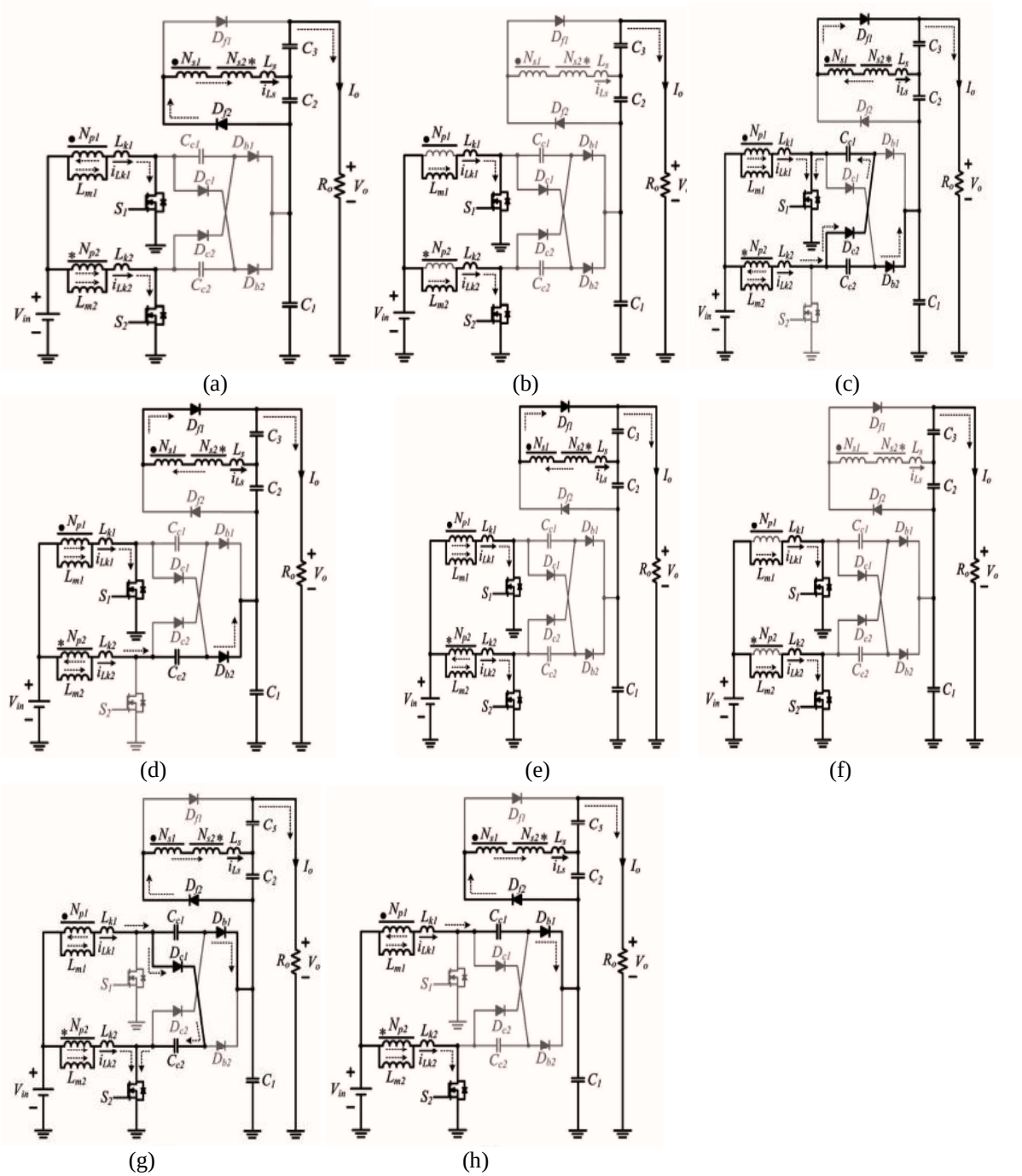

Fig 3 operating modes.

III. Steady-State Analysis

The transient characteristics of circuitry are disregarded to simplify the circuit performance analysis of the proposed converter in CCM, and some formulated assumptions are as follows.

1) All of the components in the proposed converter are ideal.

2) Leakage inductors Lk1, Lk2, and Ls are neglected.

3) Voltages on all capacitors are considered to be constant because of infinitely large capacitance

4) Due to the completely symmetrical interleaved structure, the related components are defined as the corresponding symbols such as Dc1 and Dc2 defined as Dc.

A. Step-Up:

Gain The voltage on clamp capacitor Cc can be regarded as an output voltage of the boost converter; thus, voltage VCc can be derived from

$$V_{Cc} = 1/\ 1 - D\ V_{in} \quad \ldots\ldots(1)$$

When one of the switches turns off, voltage VC1 can obtain a double output voltage of the boost converter derived from

$$V_{C1} = 1/\ 1 - D\ V_{in} + V_{Cc} = 2\ /1 - D\ V \quad \ldots\ldots\ (2)$$

The output filter capacitors C2 and C3 are charged by energy transformation from the primary side. When S2 is in ON state and S1 is in OFF state, VC2 is equal to the induced voltage of Ns1 plus the induced voltage of Ns2, and when S1 is in ON state and S2 is in OFF state, VC3 is also equal to the induced voltage of Ns1 plus the induced voltage of Ns2. Thus, voltages VC2 and VC3 can be derived from

$$V_{C2} = V_{C3} = n \cdot V_{in}\ (1 + D/\ 1 - D) = (n/\ 1 - D)\ V_{in} \quad \ldots\ldots(3)$$

The output voltage can be derived from

$$V_o = V_{C1} + V_{C2} + V_{C3} = (2n + 2\ /1 - D)\ V_{in} \quad \ldots\ldots(4)$$

In addition, the voltage gain of the proposed converter is

$$V_o\ /V_{in} = 2n + 2/\ 1 - D \quad \ldots\ldots(5)$$

Equation (5) confirms that the proposed converter has a high step-up voltage gain without an extreme duty cycle. The curve of the voltage gain related to turn ratio n and duty cycle is shown in Fig. 6. When the duty cycle is merely 0.6, the voltage gain reaches ten at a turn ratio n of one; the voltage gain reaches 30 at a turn ratio n of five.

B.Voltage Stress on Semiconductor Component:

The voltage ripples on the capacitors are ignored to simplify the voltage stress analysis of the components of the proposed converter. The voltage stress on power switch S is clamped and derived from

$$V_{S1} = V_{S2} = (2/\ 1 - D)\ V_{in} = (1/\ 2n + 2)\ V_o \quad \ldots\ldots(6)$$

Equation (6) confirms that low-voltage-rated MOSFET with low RDS (ON) can be adopted for the proposed converter to reduce conduction losses and costs. The voltage stress on the power switch S accounts for a fourth of output voltage Vo, even if turn ratio n is one. This feature makes the proposed converter suitable for high step-up and high-power applications.

The voltage stress on diode Dc is equal to VC1, and the voltage stress on diode Db is voltage VC1 minus voltage VCc. These voltage stresses can be derived from

$$V_{Dc1} = V_{Dc2} = (2/\ 1 - D)\ V_{in} = (1/\ n + 1)\ V_o \quad \ldots\ldots(7)$$

$$V_{Db1} = V_{Db2} = V_{C1} - V_{C2} = (1/\ 1 - D)\ V_{in} = (1/\ 2n + 2)\ V_o \quad \ldots\ldots(8)$$

The voltage stress on diode Db is close to the voltage stress on power switch S. Although the voltage stress on diode Dc is larger, it accounts for only half of output voltage Vo at a turn ratio n of one. The voltage stresses on the diodes are lower as the voltage gain is extended by increasing turn ratio n. The voltage stress on diode Df equals the VC2 plus VC3, which can be derived from

$$V_{Df1} = V_{Df2} = (2n/\ 1 - D)\ V_{in} = (n/n + 1)V_o \quad \ldots\ldots(9)$$

Although the voltage stress on the diode Df increases as the turn ratio n increases, the voltage stress on the diodes Df is always lower than the output voltage. The relationship between the voltage stresses on all the semiconductor components and the turn ratio n.

IV. Simulation circuits and results

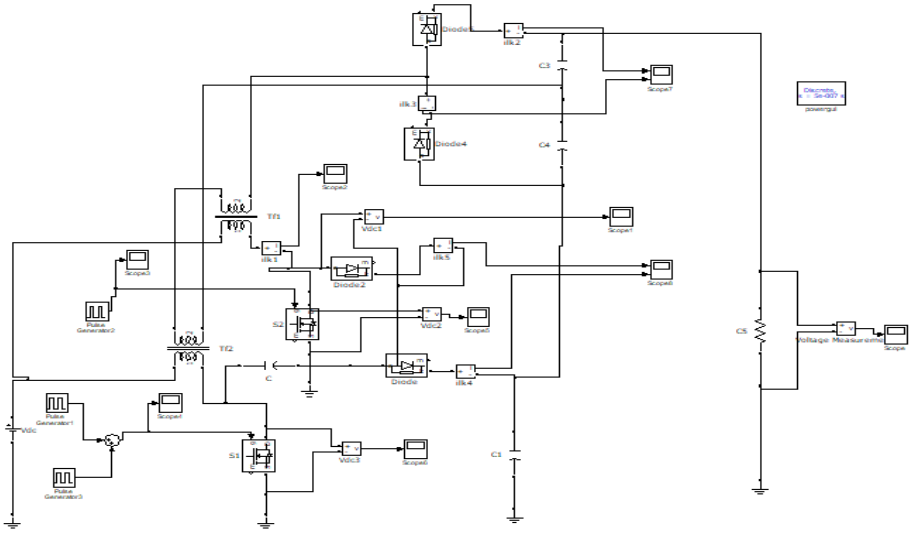

Fig 4. Simulation of interleaved converter with battery

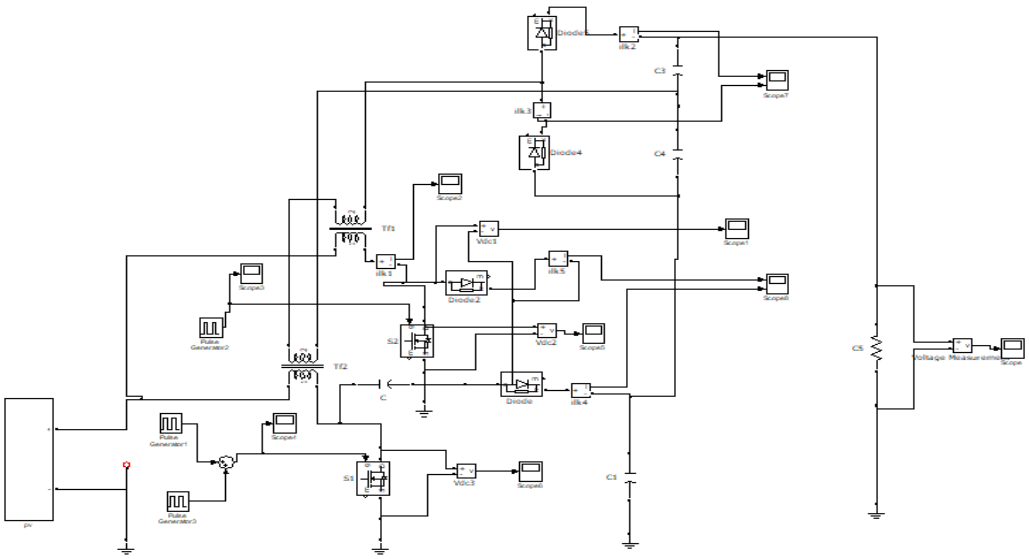

Fig 5. Simulation of interleaved converter with solar cell

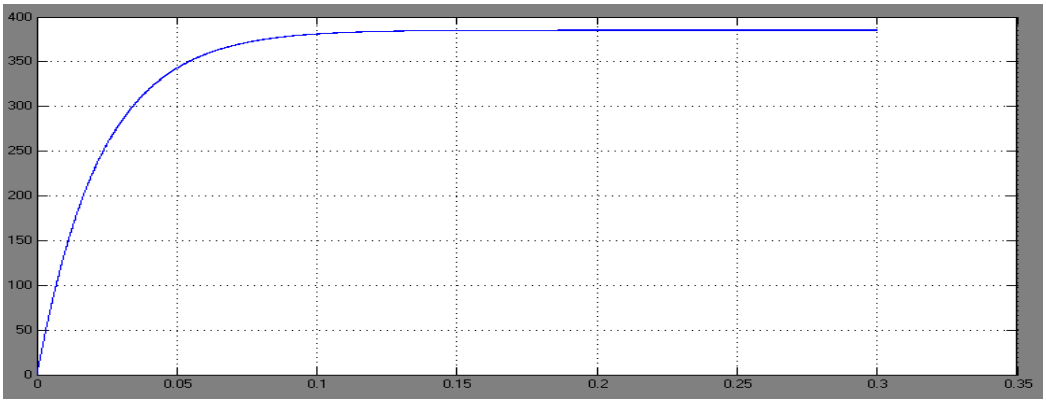

Fig. 6 DC voltage with solar cell

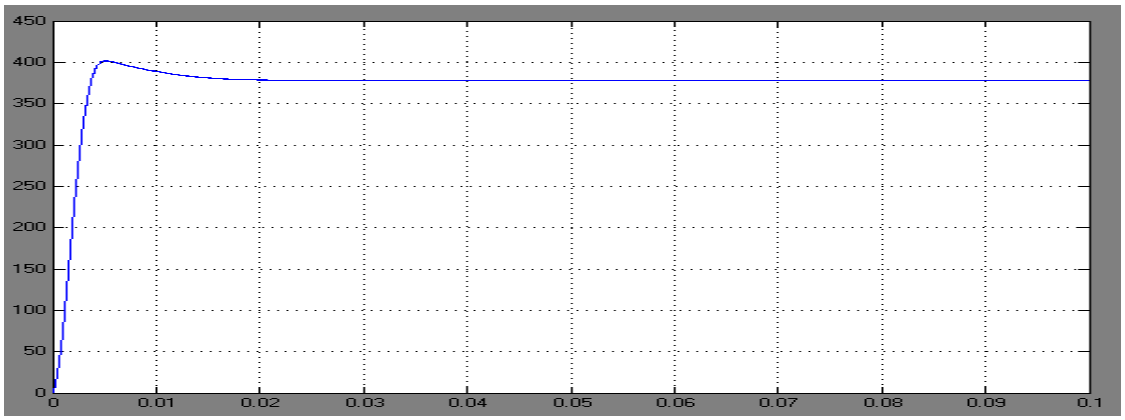

Fig. 7 DC voltage with battery cell

Dc voltage reaches to 380V with a solar source. There are less fluctuations in the output which has constant power output.

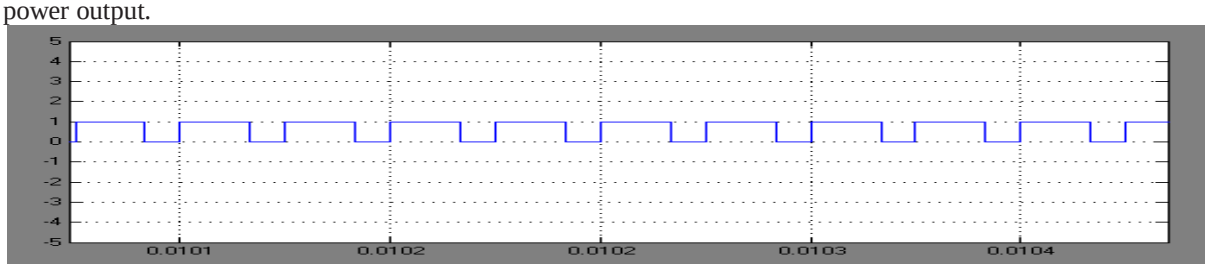

Fig 8 Pulse input switch S2

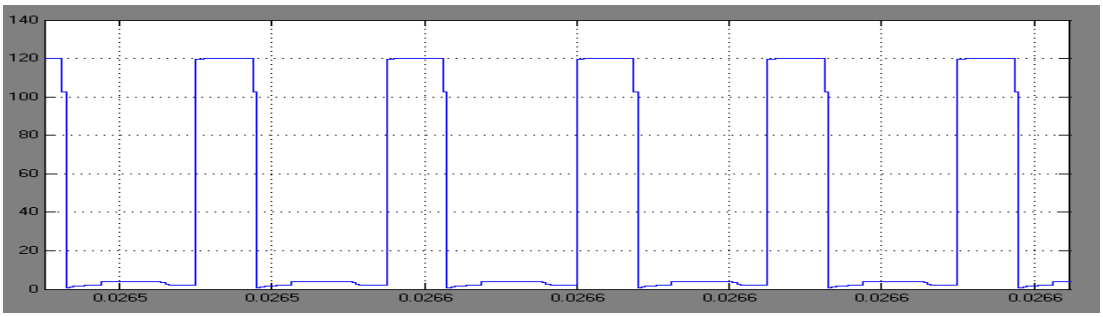

Fig 9 Voltage across power switch

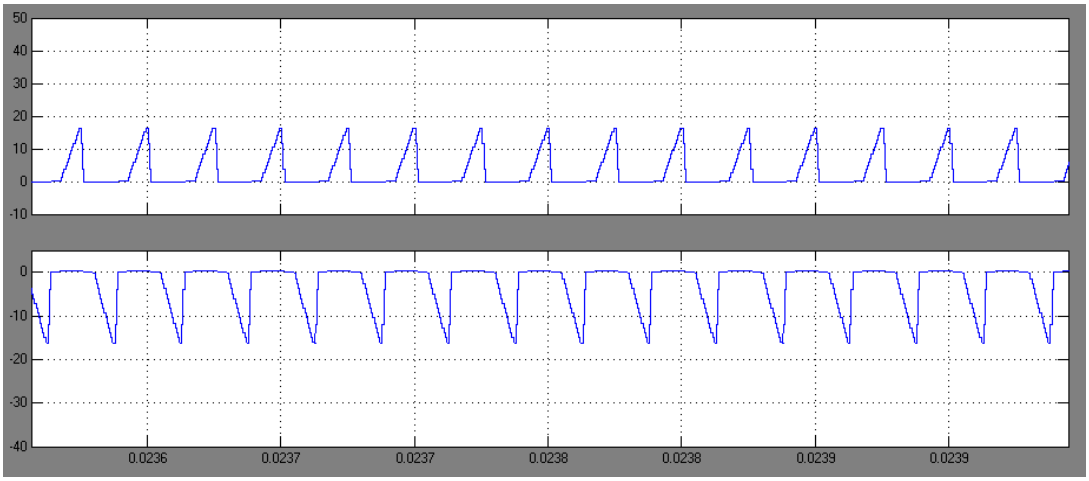

Fig. 10 Current flowing through capacitor C3

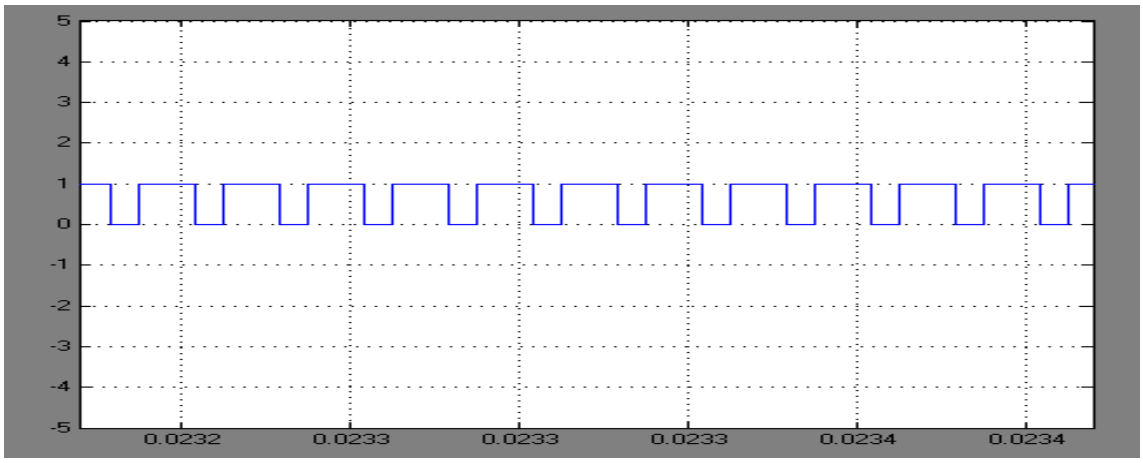

Fig 11 Pulse input switch S1

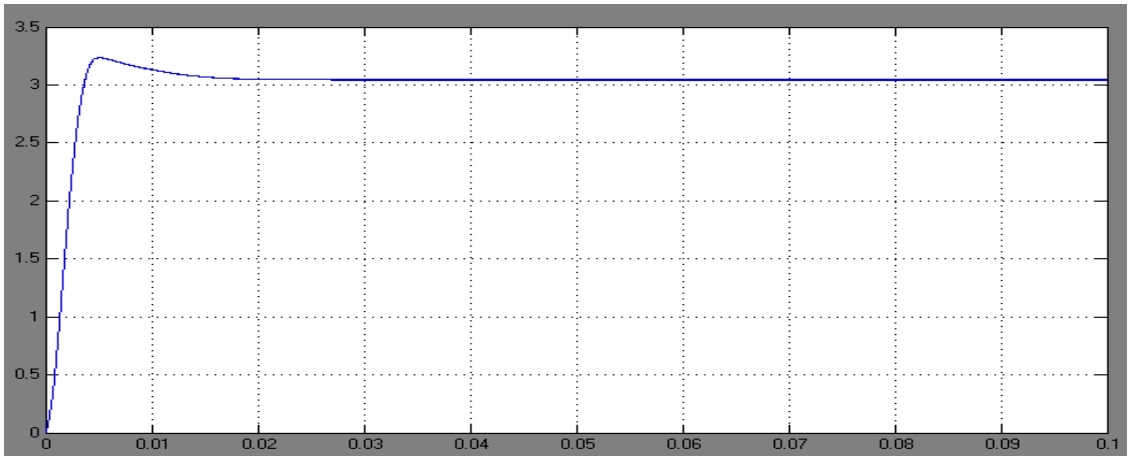

Fig 12. Output current

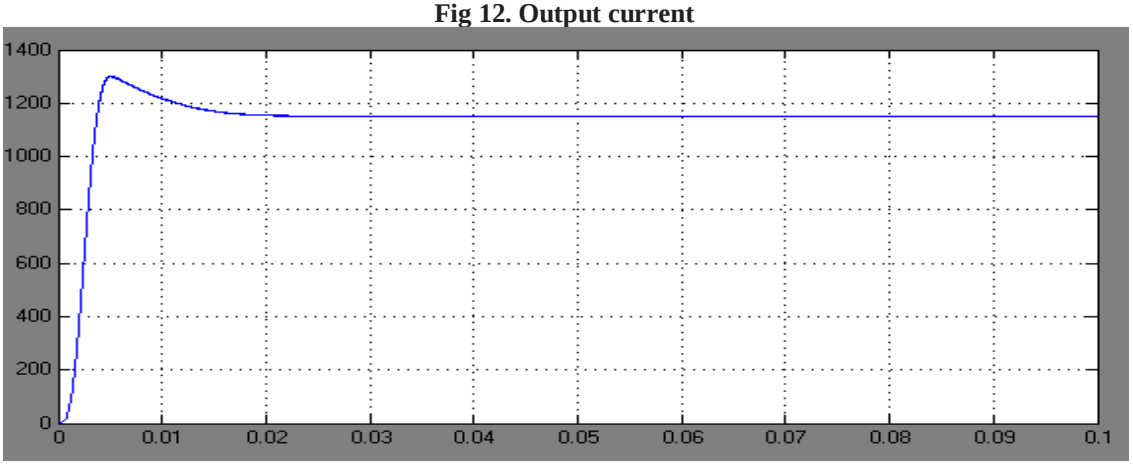

Fig 13 Output Power

V. Conclusion

This paper has presented the theoretical analysis of steady state, related consideration, simulation results for the proposed converter. The proposed converter has successfully implemented an efficient high step-up conversion through the voltage multiplier module. The interleaved structure reduces the input current ripple and distributes the current through each component. In addition, the lossless passive clamp function recycles the leakage energy and constrains a large voltage spike across the power switch. Meanwhile, the voltage stress on the power switch is restricted and much lower than the output voltage (380 V). Furthermore, the full-load efficiency is 96.4% at *Po* = 1000 W, and the highest efficiency is 97.1% at *Po* = 400 W. Thus, the proposed converter is suitable for high-power or renewable energy applications that need high step-up conversion. Maximum power output is obtained when we connect battery to the solar system as a backup.

References

[1]. J. T. Bialasiewicz, "Renewable energy systems with photovoltaic power generators: Operation and modeling," IEEE Trans. Ind. Electron., vol. 55, no. 7, pp. 2752–2758, Jul. 2008.

[2]. T. Kefalas and A. Kladas, "Analysis of transformers working under heavily saturated conditions in grid-connected renewable energy systems," IEEE Trans. Ind. Electron., vol. 59, no. 5, pp. 2342–2350, May 2012.

[3]. Y. Xiong, X. Cheng, Z. J. Shen, C. Mi, H. Wu, and V. K. Garg, "Prognostic and warning system for power-electronic modules in electric, hybrid electric, and fuel-cell vehicles," IEEE Trans. Ind. Electron., vol. 55, no. 6, pp. 2268–2276, Jun. 2008.

[4]. A. K. Rathore, A. K. S. Bhat, and R. Oruganti, "Analysis, design and experimental results of wide range ZVS active-clamped L–L type currentfed DC/DC converter for fuel cells to utility interface," IEEE Trans. Ind. Electron., vol. 59, no. 1, pp. 473–485, Jan. 2012.

[5]. T. Zhou and B. Francois, "Energy management and power control of a hybrid active wind generator for distributed power generation and grid integration," IEEE Trans. Ind. Electron., vol. 58, no. 1, pp. 95–104, Jan. 2011.

[6]. N. Denniston, A. M. Massoud, S. Ahmed, and P. N. Enjeti, "Multiplemodule high-gain high-voltage DC–DC transformers for offshore wind energy systems," IEEE Trans. Ind. Electron., vol. 58, no. 5, pp. 1877– 1886, May 2011.

[7]. H. Tao, J. L. Duarte, and M. A. M. Hendrix, "Line-interactive UPS using a fuel cell as the primary source," IEEE Trans. Ind. Electron., vol. 55, no.

[8]. 8, pp. 3012–3021, Aug. 2008. [8] K. Jin, X. Ruan, M. Yan, and M. Xu, "A hybrid fuel cell system," IEEE Trans. Ind. Electron., vol. 56, no. 4, pp. 1212–1222, Apr. 2009.

[9]. A. I. Bratcu, I. Munteanu, S. Bacha, D. Picault, and B. Raison, "Cascaded DC–DC converter photovoltaic systems: Power optimization issues," IEEE Trans. Ind. Electron., vol. 58, no. 2, pp. 403–411, Feb. 2011.

[10]. R. J. Wai, W. H. Wang, and C. Y. Lin, "High-performance stand-alone photovoltaic generation system," IEEE Trans. Ind. Electron., vol. 55, no. 1, pp. 240–250, Jan. 2008.

[11]. R. J. Wai and W. H. Wang, "Grid-connected photovoltaic generation system," IEEE Trans. Circuits Syst. I, Reg. Papers, vol. 55, no. 3, pp. 953– 964, Apr. 2008.

[12]. L. Gao, R. A. Dougal, S. Liu, and A. P. Iotova, "Parallel-connected solar PV system to address partial and rapidly fluctuating shadow conditions," IEEE Trans. Ind. Electron., vol. 56, no. 5, pp. 1548–1556, May 2009.

[13]. B. Yang, W. Li, Y. Zhao, and X. He, "Design and analysis of a gridconnected photovoltaic power system," IEEE Trans. Power Electron., vol. 25, no. 4, pp. 992–1000, Apr. 2010.

[14]. W. Li and X. He, "Review of nonisolated high-step-up DC/DC converters in photovoltaic grid-connected applications," IEEE Trans. Ind. Electron., vol. 58, no. 4, pp. 1239–1250, Apr. 2011.

[15]. C. T. Pan and C. M. Lai, "A high-efficiency high step-up converter with low switch voltage stress for fuel-cell system applications," IEEE Trans. Ind. Electron., vol. 57, no. 6, pp. 1998–2006, Jun. 2010.

[16]. R. J. Wai and R. Y. Duan, "High step-up converter with coupled-inductor," IEEE Trans. Power Electron., vol. 20, no. 5, pp. 1025–1035, Sep. 2005.

[17]. S. K. Changchien, T. J. Liang, J. F. Chen, and L. S. Yang, "Novel high step-up DC–DC converter for fuel cell energy conversion system," IEEE Trans. Ind. Electron., vol. 57, no. 6, pp. 2007–2017, Jun. 2010.

[18]. Y. P. Hsieh, J. F. Chen, T. J. Liang, and L. S. Yang, "Novel high stepup DC–DC converter with coupled-inductor and switched-capacitor techniques for a sustainable energy system," IEEE Trans. Power Electron., vol. 26, no. 12, pp. 3481–3490, Dec. 2011.

[19]. Y.-P. Hsieh, J.-F. Chen, T.-J. Liang, and L. S. Yang, "A novel high step-up DC–DC converter for a microgrid system," IEEE Trans. Power Electron., vol. 26, no. 4, pp. 1127–1136, Apr. 2011.

[20]. C. Evangelista, P. Puleston, F. Valenciaga, and L. M. Fridman, "Lyapunovdesigned super-twisting sliding mode control for wind energy conversion optimization," IEEE Trans. Ind. Electron., vol. 60, no. 2, pp. 538–545, Feb. 2013.

[21]. R. Li and D. Xu, "Parallel operation of full power converters in permanent-magnet direct-drive wind power generation system," IEEE Trans. Ind. Electron., vol. 60, no. 4, pp. 1619–1629, Apr. 2013.

[22]. L. Barote, C. Marinescu, and M. N. Cirstea, "Control structure for singlephase stand-alone wind-based energy sources," IEEE Trans. Ind. Electron., vol. 60, no. 2, pp. 764–772, Feb. 2013.

[23]. Z. Song, C. Xia, and T. Liu, "Predictive current control of three-phase grid-connected converters with constant switching frequency for wind energy systems," IEEE Trans. Ind. Electron., vol. 60, no. 6, pp. 2451– 2464, Jun. 2013.

[24]. S. M. Chen, T. J. Liang, L. S. Yang, and J. F. Chen, "A safety enhanced, high step-up DC–DC converter for AC photovoltaic module application," IEEE Trans. Power Electron., vol. 27, no. 4, pp. 1809–1817, Apr. 2012.

[25]. Q. Zhao and F. C. Lee, "High-efficiency, high step-up DC–DC converters," IEEE Trans. Power Electron., vol. 18, no. 1, pp. 65–73, Jan. 2003.

Koyyana Srinivasa Rao, et. al. "Simulation of High Step-Up Isolated Interleaved Converter for Renewable Energy System." *IOSR Journal of Electrical and Electronics Engineering (IOSR-JEEE),* 16(4), (2021): pp. 09-18.